ELSEVIER

Computers and Geotechnics 26 (2000) 199–223

COMPUTERS AND GEOTECHNICS

www.elsevier.com/locate/compgeo

Reviewing probabilistic soils modelling

R. Rackwitz *

Technical University Munich, Arcisstrasse 21, 80290 Munich, Germany

Abstract

The probabilistic approach to soils and foundation engineering requires a suitable set of models. Consistency and comparability require that these models are to a certain extent standardized but capable of incorporating the most important aspects. The concept of ergodicity is introduced as an important tool of probabilistic modelling. For layered soils some standard random field models are proposed. Their properties are discussed. Especially for soils and foundation engineering a Bayesian approach to handle different types of knowledge is mandatory — even in simplified form. An attempt is made to quantify prior information about different soil types and a simple update formula is presented. A methodology to treat classification errors is proposed. An illustrating example is presnted.

1. Introduction

Advanced probabilistic approaches to safety and reliability of structures are rather common and, in part, have penetrated already into practical applications and code making. Although the soil mechanics profession has started the study of probabilistic approaches already in the 1970s the success in theory and applications has been moderate. Three main reasons can be listed for this discrepancy.

- Most problems in soils and foundation engineering must be solved on the basis of few direct or indirect field observations.
- Many problems in soils and foundation engineering are dealt with either by simplistic mechanics, e.g. plasticity theory, or by complicated non-linear finite elements. Complicated mechanical models carry over to any reliability analysis

* Tel.: +49-89-289-23050; fax: +49-89-289-23046.

E-mail address: rackwitz@massivbau.bauwesen.tu-muenchen.de

0266-352X/00/$ - see front matter
PII: S0266-352X(99)00039-7

- Probabilistic soils modelling most frequently is a modelling by layered non-homogeneous random fields which is much more complicated than simple random variable modelling as required in most other fields of structural engineering.

Soils and foundation engineers tend to claim that the largest uncertainties are, in fact, hidden in the mechanics and essential progress in this field must still be expected in the future. A quantification of this uncertainty can only be made by experiments or, better, by field observations. This is beyond the scope of this study but it should be clear that any reliability study must include quantities which capture the uncertainty in the calculation models. In this paper some of the more common theoretical tools in probabilistic soils modelling are reviewed and discussed. A Bayesian framework for updating prior knowledge with actual observation will be set up. Only a few pieces of the theory and concept are really new (see, for example, [1–3]), but this appears to be the first time that various aspects of probabilistic soils modelling are collected in one place to form a common basis for application of modern reliability methods to soils and foundation engineering. It is proposed that these models are standard models. A certain degree of standardization with respect to the models is mandatory for all reliability analyses because their results are conditional on the models. Such standard models must obey certain requirements from an engineering point of view. A first obvious requirement is consistency. Applications enforce operational simplicity. Easy and straightforward estimability is required. These in part conflicting requirements mean that such models do not necessarily reflect nature but capture the most important aspects. The concept of ergodic and non-ergodic uncertainties is introduced. Also some data for their parameters, such as a priori information, will be proposed.

2. Probabilistic model of soils with respect to strength and stiffness properties

The following basic soil properties will be considered:

- soil density
- tangent of friction angle
- cohesion
- stiffness module

The first three items are strongly related to any type of stability analysis. A probabilistic model for the last property may help to study settlements and the like.

The point shear forces along a sliding surface is according to Mohr–Coulomb

$$\tau(\xi)\mathrm{d}s(\xi) = [(\sigma(\xi) - u(\xi))f(\xi) + c(\xi)]\mathrm{d}s(\xi) \tag{1}$$

where $f(\xi) = \tan(\varphi(\xi))$ is used, $\varphi(\xi)$ and $c(\xi)$ are friction angle and cohesion, respectively. $\sigma(\xi)$ are deterministic or random normal stresses perpendicular to the surface element $\mathrm{d}s(\xi)$ and $u(\xi)$ the (undirected) pore pressure, respectively. ξ is the

location vector. It is noted that the most interesting quantity, $\tau(\xi)$, is a scalar. In general, $\sigma(\xi)$ and $u(\xi)$ can be assumed to be independent of $f(\xi)$ and $c(\xi)$. Frequently, the quantities $\sigma(\xi)$ and $u(\xi)$ can be assumed to be deterministic. If this is not reasonable a random variable model of the form $\sigma_0\sigma(\xi)$ and $u_0u(\xi)$ with σ_0 and u_0 appropriately chosen independent random variables will suffice in most cases because both quantities generally are the result of summations so that essentially only the variability of the non-ergodic part remains (see below).

3. General — geological uncertainty and intrinsic site variability

Cohesionless and cohesive soils are distinguished which usually can be classified into various types. The properties of soils usually vary in space but differently in the vertical and horizontal direction depending on their artificial or geological deposition. Any soil property should be modelled as a random field, possibly with a mean value trend with depth.

$$X(\xi) = m_X(\xi_3) + \sigma_X(\xi_3)U(\xi) \tag{2}$$

in which

$m_X(\xi_3)$ = mean value function depending on vertical coordinate ξ_3

$\sigma_X(\xi_3)$ = standard deviation function depending on vertical coordinate ξ_3

$U(\xi)$ =a zero mean random, unit variance field with parameter ξ describing the spatial variations

$\xi = (\xi_1, \xi_2, \xi_3)^T$ = spatial coordinates.

For operational reasons the random field $U(\xi)$ should be a homogeneous normal or log-normal, centralized and standardized field. Moreover, $U(\xi)$ should be an ergodic field implying that the field becomes asymptotically independent for large separations $\Delta\xi = \xi_1 - \xi_2$. Only then operations like averaging or extreme value analysis is straightforward based on a well-established theory. Also, only in this case estimation and statistical analysis is easy. The representation of a field by non-ergodic uncertain quantities such as $m_X(\xi_3)$ and $\sigma(\xi_3)$ in Eq. (2) and ergodic quantities like $U(\xi)$, therefore, is an extremely important step in the modelling process. It is noted that true ergodicity possibly is nowhere present in nature. Ergodicity is rather a tool of modelling.

In general it suffices to assume a linear trend with depth

$$m_X(\xi_3) = A + B\xi_3 \tag{3}$$

or one uses $\zeta_3 = f(\zeta_3)$ instead of ξ_3 in order to retain linear regression theory in applications. Trends in the variance or the spatial correlation usually can be neglected but can be present, especially in ξ_3. The function of variance $\sigma^2(\xi)$, in fact,

must be determined first by regression using local averages for the local mean and the local variance. Only then can the mean value trend be removed by normal regression. A trend in the spatial correlation, after a possible trend in the mean or the variance has been removed, is normally difficult to handle. After standardization a trend in the correlation function can best be identified by plotting the cumulative number of zero crossings over the spatial parameter. If this plot is not linear a trend exists. It can be removed by an appropriate scaling (transformation) of the parameter axis. The whole procedure usually requires some iteration. The statistical errors and biases when estimating variance functions and/or correlation functions are much larger than when estimating mean value trends. Therefore, care is in order whenever true trends in the variance functions and true non-homogeneity of correlation functions has to be verified and removed.

The coefficients A and B, but primarily A, can be used to model both statistical and geological uncertainties. The coefficients must be considered as random in the sense that they, firstly, contain a usually small part of purely statistical uncertainty. Much more important is that they, secondly, also can model ignorance about the true soil type and its parameters. This uncertainty will be necessarily subjective or, if prior estimates from similar soil types are available objective, but with a relatively uninformative distribution function (see below). And clearly, those uncertainties are of non-ergodic type.

4. Random field modelling

4.1. Definitions

Homogeneous, zero mean, normal or log-normal scalar random fields are completely defined by their correlation function $R(.)$ or their two-sided spectral density function $S(.)$ for which the Wiener–Chintchin relationships are [2,3]

$$R(\Delta\xi_1, \Delta\xi_2, \Delta\xi_3) = \iiint_{\Re^3} S(\kappa_1, \kappa_2, \kappa_3) \exp(i\sum_{j=1}^{3}\kappa_j\Delta\xi_j)\mathrm{d}\kappa_1\mathrm{d}\kappa_2\mathrm{d}\kappa_3$$

$$S(\kappa_1, \kappa_2, \kappa_3) = \frac{1}{(2\pi)^3}\iiint_{\Re^3} R(\Delta\xi_1, \Delta\xi_2, \Delta\xi_3) \exp(-i\sum_{j=1}^{3}\kappa_j\Delta\xi_j)\mathrm{d}\Delta\xi_1\mathrm{d}\Delta\xi_2\mathrm{d}\Delta\xi_3 \quad (5)$$

where $\Delta\xi_i$ is the separation of two points in the i-direction and $\kappa_i = 2\pi/\Delta\xi_i$; $i = 1, 2, 3$ is the corresponding directional wave number. Here, $R(\rho_1, \rho_2, \rho_3) = E[X(\xi)X(\xi+\rho)]$ is the second moment of the considered (centralized) soil property. We note that there is always $|R_X(\Delta\xi)| \geqslant R_X(0) = \sigma^2$ and symmetry with respect to the argument, i.e. $R_X(\ldots, \Delta\xi_i, \ldots) = R_X(\ldots, -\Delta\xi_i, \ldots)$. If this is true for each argument the random field has so-called quadrant symmetry. Then, it suffices to use only positive spatial lags in the auto-covariance function and positive wave numbers and there is

$$G(\kappa) = 2^n S(\kappa) \quad (6)$$

with n the dimension and

$$\sigma^2 = \int_{-\infty}^{\infty} S(\kappa)\mathrm{d}\kappa = \int_0^{\infty} G(\kappa)\mathrm{d}\kappa \quad (7)$$

Quadrant symmetry can generally be achieved by a suitable orthogonal rotation of the coordinate system.

A random field is separable if, for example,

$$R(\Delta\xi) = R(\Delta\xi_1)R(\Delta\xi_2)R(\Delta\xi_3) \quad (8)$$

and, consequently,

$$S(\kappa) = S(\kappa_1)S(\kappa_2)S(\kappa_3) \quad (9)$$

which generally makes computations much easier. For computational convenience, the random field should at least be separable with respect to the horizontal and vertical direction in which case its correlation properties can be described by

$$R(\Delta\xi) = R(\Delta\xi_1, \Delta\xi_2)R(\Delta\xi_3) \quad (10)$$

Quite generally, if correlation functions in smaller dimensions than n are admissible, then $R(\Delta\xi^n) = R(\Delta\xi^k)R(\Delta\xi^m)$ with dimension $n = m + k$ is also admissible.

A special class of homogeneous random fields is the class of isotropic fields, that are fields whose correlation structure is invariant with respect to coordinate translations, rotations and mirror reflections. Their auto-covariance function only depends on the spatial separation $\Delta\xi = \sqrt{\Delta\xi_1^2 + \Delta\xi_2^2 + \Delta\xi_3^2}$ and their spectral density only on the wave number $\kappa = \sqrt{\kappa_1^2 + \kappa_2^2 + \kappa_3^2}$. In this case one can define radial covariance functions and radial spectral functions which are related to the original functions by

$$\sigma^2 = \int_0^{\infty} G(\kappa)\mathrm{d}\kappa = \frac{\pi^{n/2}}{2^{n-1}\Gamma(n/2)}\int_0^{\infty}\kappa^{n-1}G^R(\kappa)\mathrm{d}\kappa \quad (11)$$

$G(\kappa)$ and $G^R(\kappa)$ coincide only for $n = 1$. Isotropy implies quadrant symmetry. Radial correlation function and radial spectral function are related by the Fourier–Bessel transform

$$R_X^R(\rho) = (2\pi)^{n/2}\int_0^{\infty}\frac{J_{\frac{n-2}{2}}(\kappa\rho)}{(\kappa\rho)^{\frac{n-2}{2}}}\kappa^{n-1}G_X^R(\kappa)\mathrm{d}\kappa$$

$$G_X^R(\kappa) = \frac{1}{(2\pi)^{n/2}}\int_0^{\infty}\frac{J_{\frac{n-2}{2}}(\kappa\rho)}{(\kappa\rho)^{\frac{n-2}{2}}}\rho^{n-1}R_X^R(\rho)\mathrm{d}\rho \quad (12)$$

where $J_k(.)$ is the Bessel function of the first kind and order k and $\rho = \Delta\xi$. Note that the terms involving the Bessel function simplify to $J_o(\kappa\rho)$ and $\sin(\kappa\rho)/\kappa\rho$ in the two- and three-dimensional cases, respectively.

If an isotropic field has admissible correlation function $R^R(\Delta\xi)$, then, an anisotropic field can be generated by $R^R(\Delta\xi) = R^R(|\Delta\xi^T C\Delta\xi|)$ where C is a diagonal matrix not proportional to the identity matrix I. Such a field has an ellipsoidal correlation structure and will also be quadrant symmetric.

So far the description of standardized fields by autocorrelation functions or spectral densities are second moment descriptions and thus distribution-free. In most cases, however, the Gaussian or normal distribution is used. Then, the field is called a Gaussian or normal field.

4.2. *Special one-dimensional models*

Among the many possible forms of admissible correlation functions, six different standard one-dimensional functional forms may be used (Table 1).

$J_o(.)$ is the Bessel function of first kind and order zero, $K_b(.)$ is the modified Bessel function of second kind and order b.

All autocorrelation functions belong to ergodic fields. From Fig. 1 it is seen that the autocorrelation functions do not differ very much for small separations r. In contrast, the spectral densities, especially for model V and VI, show significant differences for small as well as for large k. The oscillating behaviour of the spectral density of model VI may discriminate it as a model describing natural fluctuations. The first two and the sixth functions belong to the class of non-differentiable processes, the next three functions to differentiable processes. The property of differentiability is usually not important because averaging operations, as common in soils engineeering, will make non-differentiable fields differentiable. Differentiability, however, will be necessary if extreme values have to be determined. The second and

Table 1
One-dimensional models for correlation function and spectral density

Type of auto-correlation function	Autocorrelation function $R(\rho)$	Spectral density function $G(\kappa)$
I	$\sigma^2 \exp[-a\lvert\rho\rvert]$	$\sigma^2 \frac{2a}{\pi(a^2+\kappa^2)}$
II	$\sigma^2 \exp[-a\lvert\rho\rvert]\cos(b\rho)$	$\frac{2\sigma^2 a(a^2+\kappa^2+b^2)}{\pi(\kappa^4+2\kappa^2(a^2-b^2)+(a^2+b^2)^2}$
III	$\sigma^2 \exp[-a\rho^2]J_0(b\rho)$	$2\int_0^\infty \sigma^2 \exp[-a\rho^2]J_0(b\rho)\cos(\kappa\rho)\mathrm{d}\rho$
IV	$\sigma^2 \exp[-a\rho^2]$	$\frac{\sigma^2}{\sqrt{\pi a}}\exp\left[-\frac{\kappa^2}{4a}\right]$
V	$\sigma^2 \frac{(a\rho)^b K_b(a\rho)}{2^{b-1}\Gamma(b)}$	$\frac{2\sigma^2\Gamma(b+1/2)a^{2b}}{\pi^{1/2}\Gamma(b)(a^2+\kappa^2)^{b+1/2}}$
VI	$\begin{cases}\sigma^2(1-\lvert\rho\rvert/a) & for \lvert\rho\rvert \geqslant a \\ 0 & for \lvert\rho\rvert > a\end{cases}$	$\frac{2}{\pi}\frac{1-\cos(a\kappa)}{a\kappa^2}$

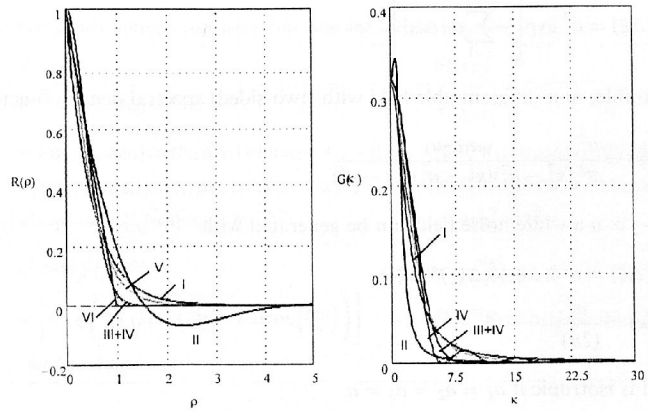

Fig. 1. One-dimensional autocorrelation functions and their spectral densities.

third functions have the form of a damped oscillation. The third to fifth functions are decaying rather rapidly. The fifth model is widely used in turbulence theory. The last function is a function with zero correlation outside a given value. Models I, IV and VI are one parameter models. The others have two parameters and the estimation problem will become more difficult. The corresponding spectra are all analytic. There is no particular physical preference to any of the proposed models. However, strength properties of non-cohesive soils show distinct Markovian behaviour and, therefore model I appears appropriate. Also, if the geological formation processes show periodic behaviour one may select model II or III. This is not to be confused with the oscillating behaviour of empirical autocorrleations functions which is purely statistical bias. Other forms of autocorrelation functions are possible, especially those generated from higher order auto-regressive processes.

Functions which are valid functions in one dimension may no more be valid (not positive definite) in higher dimensions. In particular, for isotropic fields there must be $\rho(\Delta\xi) \geqslant -1/n$ for all $\Delta\xi$. Since there is no simple relationship between $G(.)$ and $G^R(.)$ it is generally necessary to start from an admissible autocovariance or autocorrelation function and then generate the spectral function by Fourier–Bessel transforms.

The choice of one of the above models together with an assumption about the distribution function of the field makes estimation of the parameters much easier.

4.3. *3-Dimensional fields*

4.3.1. *3-Dimensional exponentially correlated fields*

The exponentially correlated field with correlation function

$$R_1(\Delta\xi) = \sigma^2 \exp\left[-\sum_{i=1}^{3} a_i|\Delta\xi_i|\right] \tag{13}$$

is a separable, non-differentiable field with (two-sided) spectral density function

$$S_X(\kappa) = \frac{\sigma^2}{\pi^3} \frac{a_1 a_2 a_3}{(\kappa_1^2 - a_1^2)(\kappa_2^2 - a_2^2)(\kappa_3^2 - a_3^2)} \tag{14}$$

For $a_i \to \infty\, a$ a white noise field can be generated with

$$R_X(\Delta\xi) = \sigma^2 \delta(\Delta\xi_1)\delta(\Delta\xi_2)\delta(\Delta\xi_3) \tag{15}$$

$$S_X(\kappa) = \frac{\sigma^2}{(2\pi)^3} \tag{16}$$

The field is isotropic if $a_1 = a_2 = a_3 = a$.

4.3.2. 3-dimensional fields with Gaussian correlation function

The field with correlation function

$$R_X(\Delta\xi) = \sigma^2 \exp\left[-\sum_{i=1}^{3} a_i \Delta\xi_i^2\right] \tag{17}$$

is a separable differentiable field with spectral density

$$S_X(\kappa) = \frac{\sigma^2}{(4\pi)^{3/2}} \frac{1}{\sqrt{a_1 a_2 a_3}} \exp\left[-\frac{1}{4}\sum_{i=1}^{3} \frac{\kappa_i^2}{a_i}\right] \tag{18}$$

The field is isotropic if $a_1 = a_2 = a_3 = a$. Both 3-dimensional models are easily generalized to n dimensions.

4.4. Horizontally isotropic fields

For horizontally isotropic fields one can use the models shown in Table 2. Note that $\Delta\xi_{12} \geqslant 0$ and $\kappa_{12} \geqslant 0$.

Note that field I is not the same as the exponentially correlated field defined by Eq. (13). While the former is separable, the latter is not because it depends on $\sqrt{\Delta\xi_1^2 + \Delta\xi_2^2}$. The three-dimensional equivalent of the (complicated) model VI has the following representation.

$$R(\Delta\xi_{123}) = \sigma^2\left[1 - \frac{3}{2}\frac{\Delta\xi_{123}}{a_{123}} + \frac{1}{2}\left(\frac{\Delta\xi_{123}}{a_{123}}\right)^3\right]$$

$$G^R(\kappa_{123}) = 12\left[\frac{\kappa_{123}^2 a_{123}^2 - 4}{\kappa_{123}^6 a_{123}^3 \pi^2}\cos(\kappa_{123}a_{123}) + \frac{4 + \kappa_{123}^2 a_{123}^2 - 4\kappa_{123}a_{123}\sin(\kappa_{123}a_{123})}{\kappa_{123}^6 a_{123}^3 \pi^2}\right] \tag{19}$$

Table 2
Models for horizontally isotropic correlation functions and spectral densities

Model	$R_X(\Delta\xi_{12})$	$G_X^R(\kappa_{12})$
I	$\sigma^2 \exp[-a_{12}\Delta\xi_{12}]$ with $a_{12} > 0$	$\frac{\sigma^2}{\pi}\frac{2a_{12}}{(a_{12}^2+\kappa_{12}^2)^{3/2}}$
II	$\sigma^2 \exp[-a_{12}\Delta\xi_{12}]\cos(b_{12}\Delta\xi_{12})$ with $a_{12} > b_{12} > 0$	$\frac{2\sigma^2}{\pi}\int_0^\infty R_X(\Delta\xi_{12})J_0(\kappa_{12}\Delta\xi_{12})\Delta\xi_{12}\mathrm{d}\Delta\xi_{12}$
III	$\sigma^2 \exp[-a_{12}\Delta\xi_{12}^2]J_0(b_{12}\Delta\xi_{12})$ with $a_{12} > 0, b_{12} > 0$	$\frac{2\sigma^2}{\pi}\int_0^\infty R_X(\Delta\xi_{12})J_0(\kappa_{12}\Delta\xi_{12})\Delta\xi_{12}\mathrm{d}\Delta\xi_{12}$
IV	$\sigma^2 \exp[-a_{12}\Delta\xi_{12}^2]$ with $a_{12} > 0$	$\frac{\sigma^2}{\pi a_{12}}\exp\left[-\frac{\kappa_{12}^2}{4a_{12}}\right]$
V	$\sigma^2 \frac{(a_{12}\Delta\xi_{12})^b K_b(a_{12}\Delta\xi_{12})}{2^{b-1}\Gamma(b)}$	$\sigma^2 \frac{4ba_{12}^{2b}}{\pi(a_{12}^2+\kappa_{12}^2)^{b+1}}$
VI	$\sigma^2\left[1 - \frac{2}{\pi}\left(\frac{\Delta\xi_{12}}{a_{12}}\sqrt{1-\left(\frac{\Delta\xi_{12}}{a_{12}}\right)^2} + \arcsin\left(\frac{\Delta\xi_{12}}{a_{12}}\right)\right)\right]$ for $\Delta\xi_{12} \leqslant a_{12}$	$\frac{2\sigma^2}{\pi}\int_0^{a_{12}} R_X(\Delta\xi_{12})J_0(\kappa_{12}\Delta\xi_{12})\Delta\xi_{12}\mathrm{d}\Delta\xi_{12}$

This correlation function is also admissible in two dimensions.

The two-dimensional isotropic fields for the horizontal variations can be combined with any of the functions for the vertical variations to obtain a valid representation of a three-dimensional field.

4.5. Correlation radius (scale of fluctuation, correlation distance, correlation length)

The correlation radius δ is defined as the width, area or volume of a rectangle, circle or sphere, respectively, with unit correlation having the same area, volume and hypervolume under the correlation function (Table 3). It thus defines a characteristic size of the field where correlation is strong. In the one-dimensional case

$$\alpha_1 = \delta_1 = \frac{2}{\sigma^2}\int_0^\infty R(\Delta\xi_i)\mathrm{d}\Delta\xi_i = \frac{1}{\sigma^2}\pi G(0) \tag{20}$$

Table 3
Correlation radius for models in Tables 1 and 2

Model	One-dimensional (vertical)	Two-dimensional (horizontal)
I	$\frac{2}{a_3}$	$\frac{2\pi}{a_{12}}$
II	$\frac{2a_3}{a_3^2+b_3^2}$	$\frac{2\pi(a_{12}^2-b_{12}^2)}{(a_{12}^2+b_{12}^2)^2}$
III	$\sqrt{\frac{\pi}{a_3}}\exp\left[-\frac{b_3^2}{8a_3}\right]I_0\left(\frac{b_3^2}{8a_3}\right)$	$\frac{\pi}{a_{12}}\exp\left[-\frac{b_{12}^2}{4a_{12}}\right]$
IV	$\sqrt{\frac{\pi}{a_3}}$	$\frac{\pi}{a_{12}}$
V	$\frac{2\sqrt{\pi}\Gamma(b+\frac{1}{2})}{a_3\Gamma(b)}$	$\frac{4\pi b_{12}}{a_{12}^2}$
VI	a_3	$1.017a_3$

If the field is separable one obtains, for example, in the two-dimensional case assuming an ellipsoidal correlation structure

$$\alpha_2 = \delta_{eq}^2 \pi = \delta_1 \delta_2 \pi = \frac{4}{\sigma^2} \int_0^\infty R(\Delta\xi_1) \mathrm{d}\Delta\xi_1 \int_0^\infty R(\Delta\xi_2) \mathrm{d}\Delta\xi_2 = \frac{1}{\sigma^2} \pi^2 G(0,0) \tag{21}$$

For isotropic fields there is only one such measure

$$\alpha_2 = \pi\delta_2^2 = \frac{2\pi}{\sigma^2} \int_0^\infty \Delta\xi_{12} R(\Delta\xi_{12}) \mathrm{d}\Delta\xi_{12} = \frac{\pi^2 G(0,0)}{\sigma^2} = \frac{\pi^2 G^R(0)}{\sigma^2} \tag{22}$$

in two dimensions and

$$\alpha_3 = \frac{4}{3}\pi\delta_3^3 = \frac{4\pi^2}{\sigma^2} \int_0^\infty \Delta\xi_{123}^2 R(\Delta\xi_{123}) \mathrm{d}\Delta\xi_{123} = \frac{\pi^3}{\sigma^2} G(0,0,0) = \frac{\pi^3}{\sigma^2} G^R(0) \tag{23}$$

in three dimensions provided that the integral $\int_0^\infty \rho^k R(\rho) \mathrm{d}\rho$ exists. The correlation radius can be interpreted as a scalar measure of the average spatial extension of the field where the correlation is strong. In fact, it has been frequently suggested to model a random field by a field which has correlation one inside the correlation radius and zero outside.

$I_o(\cdot)$ is the modified Bessel function of first kind and order zero. The three-dimensional correlation radii are computed correspondingly. All correlation parameters are analytic. The estimation of the correlation parameters from field measurements is best be done by the method of least squares. From the correlation parameters α_i representing a length, area or volume, respectively, the corresponding correlation radii δ_i can be computed. It is noted that a definition sometimes found in the literature defining the "correlation length" as the length where the correlation function falls off to $\exp(-1)$ is an inferior definition — especially in higher dimensions, compared with the definition above that the correlation radius is a scalar measure of the distance where correlation is strong. It is also noted that alternative definitions exist. The correlation radius (in one dimension) sometimes, for example, in turbulence theory, is defined as

$$\alpha_1' = \delta_1' = \frac{1}{\sigma^2} \int_0^\infty R(\Delta\xi_i) \mathrm{d}\Delta\xi_i = \frac{1}{2\sigma^2} \pi G(0) \tag{24}$$

and correspondingly in higher dimensions.

4.6. Log-normal fields and other non-gaussian fields

A log-normal field can be generated from a normal field by an appropriate transformation. The original field is represented by

$$X(\xi) = \exp[U(\xi)\delta_X + \eta_X] \tag{25}$$

with $\delta_X^2 = \ln(1+V_X^2)$, $\eta_X = \ln(m_X) - \frac{1}{2}\delta_X^2$ and $V_X = \frac{\sigma_X}{m_X}$ and where $U(\xi)$ is a zero mean, unit standard deviation normal field. The equivalent correlation function is

$$\rho_X(\Delta\xi) = \frac{(1+V_X^2)^{\rho_U(\Delta\xi)} - 1}{V_X^2} \quad \text{or} \quad \rho_U(\Delta\xi) = \frac{\ln(\rho_X(\Delta\xi)V_X^2 + 1)}{\ln(V_X^2+1)} \tag{26}$$

from which it follows that $\rho_X(\Delta\xi)$ be such that $\rho_X(\Delta\xi)V_X^2 < -1$. Otherwise the equivalent autocorrelation functions $\rho_U(\Delta\xi)$ are no longer positive definite. Restrictions, therefore, must be imposed on the parameter b for the second and third univariate correlation functions in Table 1. Other non-Gaussian fields can also be generated on similar lines [4]. The Nataf model assumes that the original variable X can be transformed into a standard normal variable, i.e. by

$$u = \Phi^{-1}[F_X(x)]$$

Let u_1 and u_2 be the transformed variables at spatial distance $\Delta\xi$. The correlation function of the transformed field must be obtained from the integral equation

$$\rho_X(\Delta\xi) = \int_{-\infty}^{+\infty}\int_{-\infty}^{+\infty} \left[\frac{F_X^{-1}(\Phi(u_1)) - m_X}{\sigma_X}\right]\left[\frac{F_X^{-1}(\Phi(u_2)) - m_X}{\sigma_X}\right] \varphi_2(u_1, u_2 : \rho_U(\Delta\xi))\mathrm{d}u_1\mathrm{d}u_2$$

$\varphi(.,.,.)$ is the bivariate standard normal density. The equation must be solved for $\rho_U(\Delta\xi)$ for any given $\rho_X(\Delta\xi)$. In a few cases the integral is analytic [5]. Otherwise a numerical solution must be sought. Again, the function $\rho_U(\Delta\xi)$ must be positive definite which imposes rather severe restrictions on the original distribution function and/or the type of $\rho_X(\Delta\xi)$.

4.6.1. Cross-correlations between components of property vector

The components of $X(\xi)$ may be independent or dependent. Then, in general, it must be assumed that for any ξ the correlation matrix is

$$R = \begin{bmatrix} \rho_{11} & \rho_{12} & \cdots & \rho_{1r} \\ \rho_{21} & \rho_{22} & \cdots & \rho_{2r} \\ \vdots & \vdots & \ddots & \vdots \\ \rho_{r1} & \rho_{r2} & \cdots & \rho_{rr} \end{bmatrix} \tag{27}$$

For normal-lognormal fields there is

$$\mathrm{Cov}[\ln(X_i), \ln(X_j)] = \ln\left[1 + \frac{\mathrm{Cov}[X_i, X_j]}{m_{X_i} m_{X_j}}\right] \tag{28}$$

$$\mathrm{Cov}[X_i, \ln(X_j)] = \frac{\mathrm{Cov}[X_i, X_j]}{m_{X_j}} \tag{29}$$

A generic element of the correlation function matrix has the form

$$R_{X_i X_j}(\Delta\xi) = \rho_{ij} R(\Delta\xi) \tag{30}$$

implying that all soil properties have the same spatial correlation structure. Observations and geological considerations indicate that this is true in good approximation.

4.7. Spatial averaging of homogeneous fields

4.7.1. Analytical approach for averages along coordinate axis

There is always a certain amount of local spatial averaging when observing a homogeneous random field. Averaging over a distance L, an area A with side lengths L_1 and L_2 or a volume V with side length L_1, L_2 and L_3 yields the mean of the average while the variance of a quadrant symmetric field is

$$\begin{aligned}\mathrm{Var}[I_L] =& \frac{2^n}{L_1 L_2 \dots L_n} \int_0^{L_1}\int_0^{L_2}\dots\int_0^{L_n} \left(1-\frac{\xi_1}{L_1}\right)\left(1-\frac{\xi_2}{L_2}\right)\dots\left(1-\frac{\xi_n}{L_n}\right) \\ & C_X(\xi_1, \xi_2, \dots, \xi_n)\mathrm{d}\xi_1\mathrm{d}\xi_2\dots\mathrm{d}\xi_n \\ =& \frac{2^n\sigma_X^2}{L_1 L_2 \dots L_n} \int_0^{L_1}\int_0^{L_2}\dots\int_0^{L_n} \left(1-\frac{\xi_1}{L_1}\right)\left(1-\frac{\xi_2}{L_2}\right)\dots\left(1-\frac{\xi_n}{L_n}\right) \\ & \rho_X(\xi_1, \xi_2, \dots, \xi_n)\mathrm{d}\xi_1\mathrm{d}\xi_2\dots\mathrm{d}\xi_n \\ =& \sigma_X^2 \gamma(L_1 L_2 \dots L_n)\end{aligned} \tag{31}$$

where $\gamma(.)$ is termed variance function [2]. This variance function decays with L_1, $L_2, \dots L_n$ and simplifies for large L_1, $L_2, \dots L_n$. In particular, it is

$$\begin{aligned}\gamma(L_1 L_2, \dots, L_n) =& \frac{2^n}{L_1 L_2 \dots L_n} \int_0^{L_1}\int_0^{L_2}\dots\int_0^{L_n} \left(1-\frac{\xi_1}{L_1}\right)\left(1-\frac{\xi_2}{L_2}\right)\dots\left(1-\frac{\xi_n}{L_n}\right) \\ & \rho_X(\xi_1, \xi_2, \dots, \xi_n)\mathrm{d}\xi_1\mathrm{d}\xi_2\dots\mathrm{d}\xi_n \\ \leqslant& \frac{2^n}{L_1 L_2 \dots L_n} \int_0^{\infty}\int_0^{\infty}\dots\int_0^{\infty} \rho_X(\xi_1, \xi_2, \dots, \xi_n)\mathrm{d}\xi_1\mathrm{d}\xi_2\dots\mathrm{d}\xi_n \\ =& \frac{\alpha_n}{L_1 L_2 \dots L_n}\end{aligned} \tag{32}$$

Quite in general, for $D = \prod_{i=1}^{n} L_i$, the variance function can be approximated by

$$\gamma(D) \approx \begin{cases} 1 \text{ for } D \leqslant \alpha_n \\ \dfrac{\alpha_n}{D} \text{ for } D > \alpha_n \end{cases} \tag{33}$$

For the correlation functions given in Table 1 the one-dimensional variance functions are given in Table 4 and Fig. 2. Closed form integration formulae over surfaces in higher dimensions are complicated if available at all.

If the random field is separable there is, of course,

$$\gamma(L_1, L_2, \dots, L_n) = \gamma(L_1)\gamma(L_2)\cdots\gamma(L_n) \tag{35}$$

This relationship is especially useful when the correlation function for the horizontal field is separable from the one in the vertical direction.

Local averages of Gaussian fields are, of course, normally distributed. According to the Central Limit Theorem local averages of non-Gaussian fields tend to the normal distribution for large averaging distances L, say for $L > 5\alpha$, at least for the ergodic fields discussed herein. The assessment of distributional characteristics for shorter averaging distances is difficult [6] and not yet practical.

4.7.2. Numerical approach

Unfortunately, the semi-analytical formulae and approximations for spatial averages can not be used in many applications because the averaging direction is hardly parallel to the coordinate axes. It is also rarely possible to rotate the coordinate axes such that the foregoing results become applicable.

For a general surface with sufficiently small surface elements and $\tau(\xi)$ pointing in a certain direction, the point shear force on a surface element for use in a numerical analysis is:

$$\tau(\xi)\Delta s(\xi) = [(\sigma(\xi) - u(\xi))f(\xi) + c(\xi)]\Delta s(\xi) \tag{36}$$

Table 4
Exact one-dimensional spatial variance functions for models in Table 1

Model	$\gamma(L_1)$
I	$\frac{2(a_1L_1-1+\exp(-a_1L_1))}{(a_1L_1)^2}$
II	$2\frac{(a_1^3L_1+a_1L_1b_1^2-a_1^2+b_1^2)}{(a_1^2+b_1^2)^2L_1^2} + +2\frac{\exp(-a_1L_1)[a_1^2\cos(L_1b_1)-b_1^2\cos(L_1b_1)-2a_1b_1\sin(L_1b_1)]}{(a_1^2+b_1^2)^2L_1^2}$
III	Numerical
IV	$\frac{(\sqrt{\pi}a_1L_1\mathrm{erf}(\sqrt{a_1}L_1)-1+\exp(-a_1L_1^2))}{a_1L_1^2}$
V	Numerical
VI	$1-\frac{L_1}{3a_1}$ for $L_1 \leqslant a_1$ $\left(\frac{a_1}{L_1}\right)\left(1-\frac{a_1}{3L_1}\right)$ for $L_1 > a_1$

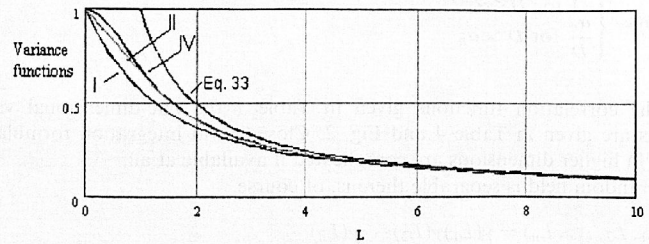

Fig. 2. Comparison of different variance functions for models in Table 1.

from which for the mean, variance and covariance, respectively

$$E[\tau(\xi)]\Delta s(\xi) \approx \{((\sigma(\xi) - u(\xi))(m_f(\xi_3) + m_c(\xi_3))\}\Delta s(\xi) \tag{37}$$

$$\mathrm{Var}[\tau(\xi)](\Delta s(\xi))^2 \approx \left\{ \begin{array}{c} (\sigma(\xi) - u(\xi))^2 \mathrm{Var}[f(\xi)] + \mathrm{Var}[c(\xi)] + \\ +(\sigma(\xi) - u(\xi))\rho_{fc} D[f(\xi)]D[c(\xi)] \end{array} \right\} (\Delta s(\xi))^2 \tag{38}$$

$$\mathrm{Cov}[\tau(\xi_1), \tau(\xi_2)](\Delta s(\xi_1))(\Delta s(\xi_2)) \approx \left\{ \begin{array}{c} (\sigma(\xi_1) - u(\xi_1))(\sigma(\xi_2) - p(\xi_2))R_f(\Delta\xi) + \\ +(\sigma(\xi_1) - u(\xi_1))\rho_{fc} R_{fc}(\Delta\xi) + \\ +(\sigma(\xi_2) - u(\xi_2))\rho_{fc} R_{fc}(\Delta\xi) + R_c(\Delta\xi) \end{array} \right\} (\Delta s(\xi_1))(\Delta s(\xi_2)) \tag{39}$$

with $(\xi_{11}, \xi_{12}, \xi_{13})$ and $(\xi_{21}, \xi_{22}, \xi_{23})$ the location vectors of two distinct points and $\Delta\xi = \sqrt{(\xi_{11} - \xi_{21})^2 + (\xi_{12} - \xi_{22})^2 + (\xi_{13} - \xi_{23})^2}$ the distance between those points. The appropriate size of the surface element depends on the correlation length. In general, it should be chosen not larger than half the correlation length, provided that such a size is mechanically feasible. This leads to a relatively fine discretization mesh at the expense of increased numerical effort. Also, it can be shown that the variances and covariances are generally estimated too small.

Much better results are usually obtained if averaging is performed first. In this case surface integrals need to be computed. For example, assume that the surface has the following explicit parametric representation.

$$\xi_3 = h(\xi_2, \xi_3) \tag{40}$$

For a centralized, homogeneous field we now have for the surface S

$$E[M(S)] = \frac{1}{A(S)} \int_S E[X(\xi)]\mathrm{d}S\xi = m_X \tag{41}$$

$$\mathrm{Var}[M(S)] = \frac{\sigma_X^2}{A(S)^2} \int_S \rho(\xi) dS(\xi)$$

$$= \frac{\sigma_X^2}{A(S)^2} \int_B \rho(\xi_1, \xi_2, h(\xi_1, \xi_2)) \sqrt{1 + \left(\frac{\partial h(\xi_1, \xi_2)}{\partial \xi_1}\right)^2 + \left(\frac{\partial h(\xi_1, \xi_2)}{\partial \xi_2}\right)^2} \mathrm{d}\xi_1 \mathrm{d}\xi_2 \tag{42}$$

$$\mathrm{Cov}[M_j(S_j), M_k(S_k)] = \frac{\sigma_X^2}{A(S_j)A(S_k)} \int_{B_j} \int_{B_k} \rho(\xi_{j,1}, \xi_{j,2}, h_j(\xi_{j,1}, \xi_{j,2}), \xi_{k,1}, \xi_{k,2}, h_k(\xi_{k,1}, \xi_{k,2})) \sqrt{1 + \left(\frac{\partial h_j(\xi_{j,1}, \xi_{j,2})}{\partial \xi_{j,1}}\right)^2 + \left(\frac{\partial h_j(\xi_{j,1}, \xi_{j,2})}{\partial \xi_{j,2}}\right)^2} \sqrt{1 + \left(\frac{\partial h_k(\xi_{k,1}, \xi_{k,2})}{\partial \xi_{k,1}}\right)^2 + \left(\frac{\partial h_k(\xi_{k,1}, \xi_{k,2})}{\partial \xi_{k,2}}\right)^2} \mathrm{d}\xi_{j,1} \mathrm{d}\xi_{j,2} \mathrm{d}\xi_{k,1} \mathrm{d}\xi_{k,2} \tag{43}$$

where B is the (unique) projection of the surface S onto the (ξ_1, ξ_2)-plane and

$$A(S) = \int_B \sqrt{1 + \left(\frac{\partial h(\xi_1, \xi_2)}{\partial \xi_1}\right)^2 + \left(\frac{\partial h(\xi_1, \xi_2)}{\partial \xi_2}\right)^2} \mathrm{d}\xi_1 \mathrm{d}\xi_2 \tag{44}$$

the area of S. Analytical results hardly exist and integrations have to be performed numerically. For piecewise plane surfaces substantial simplifications are possible because the derivatives of $h(\xi_1, \xi_2)$ remain constant within each plane. Further simplification can be achieved for separable fields and if the surface is parallel to one of the coordinate axis. Clearly, other parameterizations can be chosen with the corresponding alterations in the relevant fomulae. For property vectors one proceeds as in Eq. (39). Eqs. (40)–(44) are given here for the first time.

4.7.3. Prior information on various soil types

In general, the parameters such as the mean, the standard deviation and the correlation parameters of the soil under consideration must be inferred from in situ tests usually together with some prior information if classification of the soil into one of several types is possible. The purpose of classification is to enable the use of prior information collected from previous soil investigations of the same soil class. Classification here is primarily with respect to mechanical properties rather than from a geological point of view. An excellent vehicle to process actual observations together with prior information is Bayes' theorem. For simplicity it is assumed that the standard deviation of a property of a given soil class k is known but its mean is

not known. The soil properties are normally distributed. If they are assumed to be log-normally distributed the same procedures hold but for the logarithms of a property. Further, assume that the a priori distribution is uniform for a given soil class k.

$$f''(m_k|\bar{x}_n) = \frac{f(\bar{x}_n|m_k)f'(m_k)}{\int_{b_{k-1}}^{b_k} f(\bar{x}_n|m_k)f'(m_k)\mathrm{d}m_k} = \frac{\frac{\sqrt{n}}{\sigma_k}\varphi\left(\frac{\bar{x}_n - m_k}{\sigma_k/\sqrt{n}}\right)}{\left[\Phi\left(\frac{\bar{x}_n - b_{k-1}}{\sigma_k/\sqrt{n}}\right) - \Phi\left(\frac{\bar{x}_n - b_k}{\sigma_k/\sqrt{n}}\right)\right]} \tag{45}$$

where

$f''(m_k|\bar{x}_n)$ = a posteriori density of m_k

$f(\bar{x}_n|m_k)$ = likelihood function of $\bar{x}_n$ given m_k

$f'(m_k)$ = a priori density of m_k

$\bar{x}_n$ = mean of a sample of size n

b_k, b_{k-1} = upper/lower a priori boundary for m_k

It is seen that the assumption of a uniform prior distribution enables an analytical result for the a posterior density. If the standard deviation is not known, similar but more complicated formulae can be given [7].

In Eq. (45), and bearing in mind that the sample size is usually rather small, the a priori density contains much of the information available. In the following Tables 5a and b we have made an attempt to compile suitable class boundaries for some selected soil categories from many sources in the literature. The tables are meant to form the starting point of better tables or of tables of similar kind with different states of prior knowledge.

Mean properties are given as ranges for which a uniform prior distribution may be assumed. In exceptional cases both the midpoint and the boundaries can be different from those given in Table 5. The spatial fluctuations in terms of standard deviations, given their mean, vary as in Table 6.

These values are relatively small compared with the mean value variability. Sometimes, the standard deviations can be reduced by extensive site exploration and laboratory testing. It is important to note that they can only be so small because the mean varies according to Eq. (45). Sometimes the standard deviations are somewhat smaller for artificially deposited soils than in Table 6.

The correlation coefficient between specific weight and friction coefficient is slightly positive between 0 and 0.5. The correlation coefficient between friction coefficient and cohesion is negative around −0.5.

In general, the correlation radius for natural soils in the horizontal direction is about 5 to 50 times larger than in the vertical direction when predominantly horizontal deposition (and layering) is present. The vertical correlation radius has been found to be between less than 0.5 m to rarely more than 10 m. Small values for the vertical and large values for the horizontal direction are characteristic for strongly

Table 5
(a) Prior information for non-cohesive soils; (b) prior information for cohesive soils[a]

(a)

Soil type	Compaction	Mean specific weight (kN/m³) normal humidity	Mean specific weight (kN/m³) saturated	Mean friction coefficient	Stiffness (MN/m²)
Sand, gravel	Loose	15–17	17–19	0.58–0.65	30–100
Uniform grain size	Medium	16–18	18–20	0.65–0.73	50–150
	Dense	17–19	19–21	0.70–0.83	150–250
Coarse gravel, boulders	Loose	15–17	17–19	0.65–0.73	150–300
	Medium	16–18	18–20	0.70–0.83	150–300
	Dense	17–20	19–21	0.78–0.90	250–350
Sand, gravel	Loose	18–20	20–22	0.57–0.70	30–100
Non-uniform grain size	Medium	19–21	21–23	0.62–0.75	50–150
	Dense	20–22	22–24	0.70–0.85	150–250
Sand, gravel	Loose	18–20	20–22	0.57–0.70	100–300
Slightly cohesive sand	Medium	20–22	22–24	0.63–0.75	100–300
Non-uniform grain size	Dense	22–24	24–26	0.70–0.83	100–300

(b)

Cohesive soil type	Consistency	Mean specific weight (kN/m³)	Mean friction coefficient	Mean cohesion (kN/m²) consolidated	Mean cohesion (kN/m²) unconsolidated	Stiffness (MN/m²)
Anorganic cohesive soils	Soft	16–18	0.27–0.36	0–5	10–20	2–5
Plastic	Stiff	17–19	0.27–0.36	5–15	20–50	2–5
	Very stiff	20–22	0.27–0.36	10–20	50–100	2–5
Anorganic cohesive soils	Soft	17–19	0.35–0.42	0–5	0–10	4–8
Medium plastic	Stiff	18–20	0.35–0.42	5–10	15–30	4–8
	Very stiff	19–21	0.35–0.42	10–20	40–100	4–8
Anorganic cohesive soils	Soft	18–20	0.42–0.55	0–3	0–10	5–10
Weakly plastic	Stiff	19–21	0.42–0.55	0–5	10–25	5–10
	Very stiff	20–22	0.42–0.55	3–10	30–70	5–10
Boulder clay		20–24	0.52–0.64	20–30	–	200–700
Organic cohesive soils	Soft	13–18	0.24–0.28	0–3	5–15	2–5
Silt	Stiff	14–19	0.24–0.28	0–3	10–30	3–10

[a] Under water, the unit weight is reduced by 10 (kN/m³).

Table 6
Representative standard deviations

Soil property	Standard deviation
Specific weight (kN/m³)	1
Friction coefficient	0.06–0.10
Cohesion (kN/m²)	2–7
Stiffness (MN/m²)	5–10 %

cohesive soils and for non-cohesive soils with small grain size. Frequently, the correlation radii for artificially deposited soils are considerably shorter depending on the homogenization processes that took place during excavation, transport and deposition of the soil. The magnitudes of the proposed correlation radii may be taken for all properties unless site specific information is available.

All quantities refer to a reference volume (area) of about 0.5 (m³) and 0.65 (m²), respectively. The standard deviations given in Table 6 do not contain the unavoidable measurement error, which for most types of standard experiments is about 20–30% of the standard deviations given above.

4.7.4. Updating, classification and failure probabilities

This type of uncertainty is the uncertainty in classifying soil into one of the soil types in the tables above. Let a set $\{k\}$ of different layers be present with known standard deviation but unknown mean. Layer boundaries are assumed to be known. If it is possible to assign prior probabilities to each set, the failure probability of the problem is

$$P_f = \sum_{j=1}^{J} p_j'\{k\} P(V_j\{k\}) \tag{46}$$

with

$$1 = \sum_{j=1}^{J} p_j'\{k\}$$

and $V_j\{k\}$ the considered failure event. In general, it is hardly feasible to investigate the prior and posterior probabilities for all combinations in the set $\{k\}$.

Alternatively and more feasibly but also implying appreciable information about the number of soil classes present, one may wish to identify a certain or all of the soil classes from measurements. For a particular soil class the mean m_k is uniformly distributed, i.e. the prior probabilities are taken as given in the figure (Fig. 3).

Then, the failure probability is

$$P_f' = \sum_{k=1}^{K} p_k' P_f(V_k) \tag{47}$$

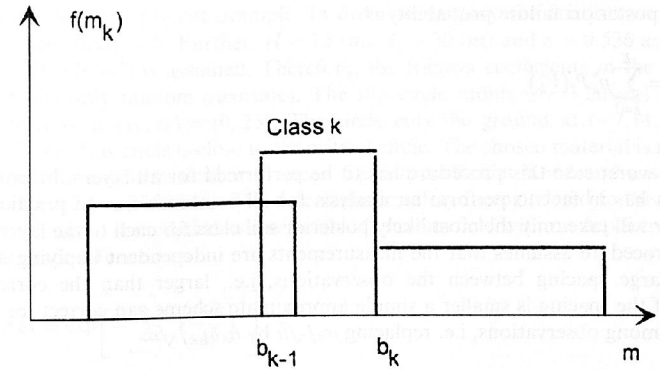

Fig. 3. Prior densities of mean for different soil classes.

in which p_k' are the prior probabilities for soil class k in a specific layer. For the soil property under investigation a normal distribution with known standard deviation is assumed. If the classification were correct the updated (posterior) mean has density [see Eq. (45)]

$$f''(m_k|\bar{x}_n) = \frac{f(\bar{x}_n|m_k)f'(m_k)}{\int_{b_{k-1}}^{b_k} f(\bar{x}_n|m_k)f'(m_k)\mathrm{d}m_k} = \frac{\frac{\sqrt{n}}{\sigma_k}\varphi\left(\frac{m_k-\bar{x}_n}{\sigma_k/\sqrt{n}}\right)}{\Phi\left(\frac{b_k-\bar{x}_n}{\sigma_k/\sqrt{n}}\right)-\Phi\left(\frac{b_{k-1}-\bar{x}_n}{\sigma_k/\sqrt{n}}\right)} \tag{48}$$

with truncated distribution function

$$F''_{\text{truncated}}(m_k|\bar{x}_n) = \frac{\Phi\left(\frac{m_k-\bar{x}_n}{\sigma_k/\sqrt{n}}\right)-\Phi\left(\frac{b_{k-1}-\bar{x}_n}{\sigma_k/\sqrt{n}}\right)}{\Phi\left(\frac{b_k-\bar{x}_n}{\sigma_k/\sqrt{n}}\right)-\Phi\left(\frac{b_{k-1}-\bar{x}_n}{\sigma_k/\sqrt{n}}\right)} \tag{49}$$

Note that correct classification means that m_k can, in fact, fall only in between the boundaries $[b_{k-1}, b_k]$. The probabilities of class k being true become

$$p''(k, \bar{x}_n \in [b_{k-1}, b_k]) = \frac{p'(k)\int_{b_{k-1}}^{b_k} P(\bar{x}_n \in [b_{k-1}, b_k]|m_k)f'(m_k)\mathrm{d}m_k}{\sum_{k=1}^{K} p'(k)\int_{b_{k-1}}^{b_k} P(\bar{x}_n \in [b_{k-1}, b_k]|m_k)f'(m_k)\mathrm{d}m_k} \tag{50}$$

where

$$\int_{b_{k-1}}^{b_k} P(\bar{x}_n \in [b_{k-1}, b_k]|m_k)f'(m_k)\mathrm{d}m_k = \Phi\left(\frac{\bar{x}_n-b_{k-1}}{\sigma_k/\sqrt{n}}\right)-\Phi\left(\frac{\bar{x}_n-b_k}{\sigma_k/\sqrt{n}}\right) \tag{51}$$

The a posteriori failure probability is

$$P_f'' = \sum_{k=1}^{K} p_k'' P_f(V_k'') \tag{52}$$

In the worst case this procedure has to be performed for all layers. In principle, one then has in fact to perform an analysis for all combinations. In practice, one probably will take only the most likely posterior soil class for each of the layers. The above procedure assumes that the measurements are independent implying a sufficiently large spacing between the observations, i.e., larger than the correlation radius. If the spacing is smaller a simple approximate scheme can correct for correlations among observations, i.e. replacing $\sigma_k/\sqrt{n}$ by $\sigma_k \delta_{1,k}/\sqrt{n}$.

4.7.5. Illustrative example

In this section we illustrate the material proposed before. As an example we take embankment stability. Bishop's widely used slip circle method is used [8]. The failure condition can be written as:

$$g(X) = rL\left(\sum_{i=1}^{m}\left\{\frac{c_i + t_i(\gamma_i h_i - u_i)}{\cos(\theta_i) + \sin(\theta_i)t_i} v_i + (V_i - V_{i+1})\right\} - \sum_{i=1}^{m} v_i h_i \gamma_i \sin(\theta_i)\right) + \text{end effects} \leqslant 0 \tag{53}$$

where:

r	= radius of slip circle
L	= length of rupture zone
c_i	= effective average cohesion in ith slice
t_i	= tan (ϕ_I) = effective average friction coefficient in ith slice
h_i	= height of ith slice
v_i	= breadth of ith slice
u_i	= average pore pressure in ith slice
γ_i	= average bulk density in ith slice
θ_i	= location angle of ith slice measured counter clockwise from negative z-axis
$V_i - V_{i+1}$	= net vertical shear forces which are set equal to zero for simplification
end effects	= two stabilizing moments from end surfaces of slip cylinder
H	= embankment height
ε	= slope angle

The simplification of setting $V_i - V_{i+1} = 0$, i.e. a possible local violation of equilibrium conditions, can be removed at the expense of additional iteration. Detailed probabilistic analyses of the slope stability problem can be found in the relevant rather rich literature. A fairly exhaustive study has been presented in [9], which is also the basis of the present example. In order to simplify the analysis we assume $c_i = u_i =$ end effects $= 0$. Further, $H = 15$ (m), $L = 30$ (m) and $\varepsilon = 0.526$ as well as $\gamma_i = \gamma = 20$ (kN/m^3) is assumed. Therefore, the friction coefficients in the various slices are the only random quantities. The slip circle radius is $r = 26$ (m) and the circle center is at $(y_0, z_0) = (0, 25)$. The circle cuts the ground at $(-7.14, 0)$ and $(23.35, 13.56)$. This circle is close to the critical circle. The chosen material is medium compacted non-uniform sand with mean friction coefficient 0.662 and a standard deviation 0.087 (see Table 5a). The deterministic safety factor related to the mean is 1.32. The material is modelled as a separable Gaussian field without depth trend and auto-correlation function

$$\rho(\Delta\xi) = \exp\left[-\sum_{i=x,y,z}^{3}\left(\frac{\Delta\xi_i}{b_i}\right)^2\right]$$

as in Eq. (17). As standard case we choose $b_z = 2$ (m) and $b_y = b_x = 5b_z$ with correlation length $\alpha_I = \sqrt{\pi} b_I$ equal to 3.55 (m), 17.73 (m) and 17.73 (m), respectively, in accordance with the above remarks. The slip circle as it cuts the ground is subdivided into m equally large sections. For this illustration we have selected $m = 10$ which has been found sufficient. At first, we need to determine the variances. In the x-direction the result for model IV in Table 4 is valid. For the other two directions we choose the following parametric representation $\xi_2 = \xi_2$ and $\xi_3 = a_k\,\xi_2 + z_{0,k}$ with $a_k = \tan(\alpha_k)$ (see Fig. 4). Application of Eq. (42) yields

$$\begin{aligned}
\mathrm{Var}[M(S_k)] &= \frac{\sigma_X^2}{L^2}\left(\sqrt{\pi} b_x \mathrm{erf}\left(\frac{L}{b_x}\right) + b_x^2\left\{1 - \exp\left[-\left(\frac{L}{b_x}\right)^2\right]\right\}\right) \\
&\times \frac{1 + a_k^2}{A(S_k)^2}\int_{y_k - \frac{v_k}{2}}^{y_k + \frac{v_k}{2}}\int_{y_k - \frac{v_k}{2}}^{y_k + \frac{v_k}{2}} \exp\left[-\frac{(\xi_1 - \xi_2)^2}{b_y^2} - \frac{(\xi_1 a_k + z m_k - (\xi_2 a_k + z m_k))^2}{b_z^2}\right] \mathrm{d}\xi_1 \mathrm{d}\xi_2 \\
&= \frac{\sigma_X^2}{L^2}\left(\sqrt{\pi} b_x \mathrm{erf}\left(\frac{L}{b_x}\right) + b_x^2\left\{1 - \exp\left[-\left(\frac{L}{b_x}\right)^2\right]\right\}\right) \\
&\times \frac{1}{v_k^2}\frac{b_y b_z}{b}\left[\sqrt{\pi b} v_k \mathrm{erf}\left(v_k \frac{b}{b_y b_z}\right) - b_y b_z\left(1 - \exp\left[-\frac{v_k^2 b}{b_y b_z}\right]\right)\right]
\end{aligned} \tag{54}$$

with $b = b_z^2 + a_k^2 b_y^2$ and $A(S_k) = \sqrt{1 + a_k^2} v_k^2$.

This is slightly more complex than the formula along a coordinate axis for model IV in Table 4. For the covariances [see Eq. (43)] we associate the first integral with the first polygonal plane and the second integral with the second polygonal plane. It is, in fact, possible to reduce the double integral into four bivariate normal integrals which in turn can be reduced to simple integrals [10]. However, the formulae are

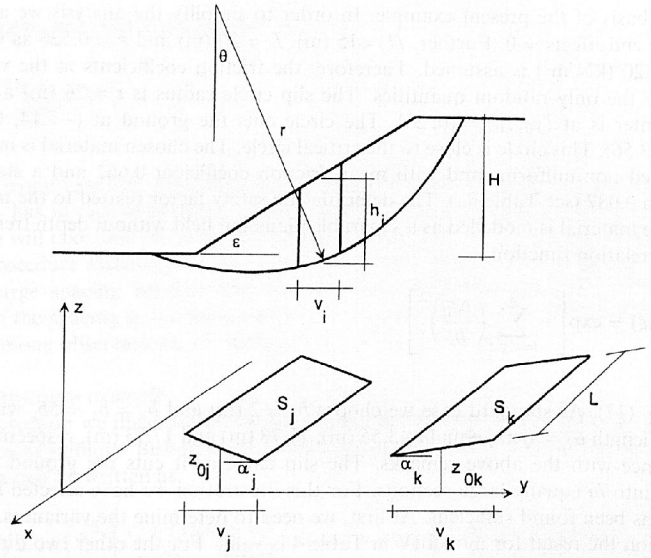

Fig. 4. Geometry of slip circle and polygonal planes.

complicated and a two-dimensional numerical integration will do as well. For other auto-correlation functions one proceeds similarly.

All further reliability analyses are performed with FORM/SORM (see, for example, [11–13]). Characteristic for these methods is that they can handle random variables and so are consistent with Bishop's discretized mechanical model. We shall now demonstrate:

1. Influence of correlation length
2. Influence of type of auto-correlation function [Eq. (13) and (17)]
3. Influence of prior information on mean friction coefficient from Table 5a
4. Influence of updating of prior information by samples
5. Influence of classification errors

Fig. 5 shows some results for two correlation settings, i.e. $b_x = b_y = 5$ and $b_x = b_y = 10b_z$, respectively. It is seen that the vertical correlation parameter b_z plays a dominating role. Also, the type of autocorrelation function is of certain importance. The exponential function Eq. (13) decays faster than the Gaussian function Eq. (17) for smaller $\Delta\xi$. Therefore, the safety indices are generally larger for the exponential function under our size conditions (Table 7). Very large $b_z (b_z > 10)$ produce numerical instabilities and singularities because the variables become highly correlated and the Choleski-scheme used here for decorrelating the

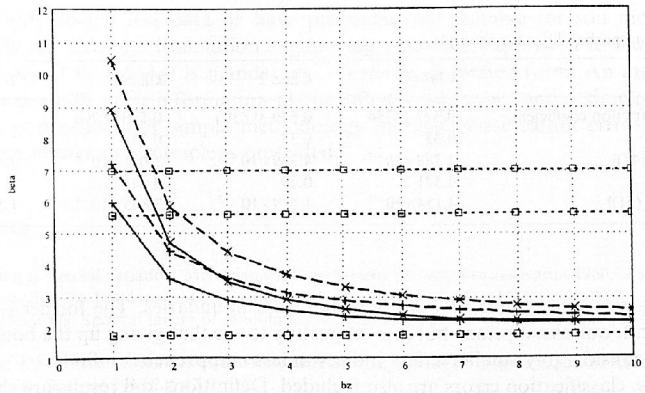

Fig. 5. Safety index versus (soil lines for Gaussian autocorrelation function, dashed lines for exponential autocorrelation function, upper lines for $b_x = b_y = 5b_z$, lower lines for $b_x = b_y = 10b_z$, lower dotted line for fully correlated variables, two upper dotted lines for uncorrelated variables).

shear forces fails. The curves approach the line for fully correlated shear forces which is computed by using the same random friction coefficient in each slice. For the independent variable case a variance reduction has been performed for the shear force in each slice. The average breadth of a slice is 3 (m), which is roughly the corresponding correlation length in this case.

The FORM-results have been checked by the more accurate SORM-procedure because due to the tan(.)-term in Eq. (53) the failure surface must be non-linear. For the standard case it is $\beta_{\mathrm{FORM}} = 7.003$ whereas $\beta_{\mathrm{SORM}} = 6.493$. For our purposes the agreement is sufficiently good but actual applications should probably always be run with SORM or even a higher order method.

We assume that the classification is correct and the class boundaries for the friction coefficient are [0.577, 0.754] (see Table 5a). Without any field sample the safety index now is 4.946 compared with 7.033 for fixed friction coefficient. If samples are taken having the sample mean at 0.662 one obtains the following results using either Eq. (45) (untruncated distribution of m_k, i.e. with the denominator neglected) or Eq.

Table 7
Safety indices versus sample size for example

n	Truncated	Not truncated
1	4.982	2.437
2	5.021	3.258
3	5.079	3.793
5	5.209	4.483
10	5.507	5.348
∞	7.033	7.033

Table 8
Total failure probabilities for example

	Class 1	Class 2	Class 3	Σ
Range of friction coefficient	0.577–0.754	0.649–0.839	0.510–0.700	
p_i'	0.33	0.33	0.33	1
p_f' [in Eq. (47)]	3.788×10^{-7}	4.349×10^{-11}	1.021×10^{-3}	3.405×10^{-4}
p_i''	0.371	0.29	0.34	1
P_f'' [in Eq. (51)]	4.154×10^{-7}	1.529×10^{-12}	3.855×10^{-4}	1.312×10^{-4}

(45) with truncated range of validity at the class boundaries. The former is inconsistent with our assumptions but it is interesting to see that giving up the boundaries leads to considerably smaller safety indices unless n approaches infinity.

Finally, classification errors are also included. Definitions and results are shown in Table 8. The prior weights are all equal. The ranges of the friction coefficients in the different classes are rather arbitrary. The posterior weights and corresponding failure probabilities are computed assuming one experiment with friction coefficient 0.662. This falls in between all class boundaries. Assuming a uniform distribution of the mean friction coefficient within the class boundaries quite different failure probabilities are obtained. Clearly, class 3 gives the largest failure probability a priori and a posteriori. The a posteriori weights differ only a little from the a priori weights. Note that class 1 is the most likely given the sample because the experiment falls close to the middle of the class range while it falls close to one of the boundaries for the other two classes. If, in fact, a (much) larger sample were taken with the same mean of experimental results class 1 would become dominant.

The prior values are computed assuming a uniform distribution of the mean friction coefficient. It should be mentioned that these results are valid only for the assumed geometry of the slip cylinder and its length along the embankment. Each modification of the property vector changes the most critical geometric parameters. Nevertheless, the example demonstrates that actual local information is extremely important. Tables of the type as in Table 5a or b can only serve for first estimates. It is also inferred from Table 8 that starting from diffuse priors for the class weights can require a considerable amount of local samples.

5. Summary and conclusions

The probabilistic approach to soils and foundation engineering requires a suitable set of models. Consistency and comparability require that these models are to a certain extent standardized but capable of incorporating the most important aspects. The concept of ergodicity is introduced as an important tool of probabilistic modelling. For layered soils some standard random field models are proposed. Their properties are discussed. Other models have been excluded from discussion on purpose because, for example, they contain more parameters that can usually be determined from limited test data or have properties not suitable for soil modelling. Especially for soils and foundation engineering a Bayesian approach to handle different types of knowledge is mandatory — even in simplified form. An attempt is made to quantify prior information about different soil types and a simple update formula is presented. A simple methodology to treat classification errors is proposed. An illustrating example is presented.

References

[1] Matern B. Spatial variation. Meddelanden Fran Statens Skogsforskningsinstitut 1960;49:5.
[2] Vanmarcke EH. Random fields — analysis and synthesis. Cambridge: MIT Press, 1983.
[3] Yadrenko MI. Spectral theory of random fields. Springer, New York: Optimization Software Publ, 1983.
[4] Nataf AD. Determination des distribution dont les marges sont donnés. Comptes Rendus de l'Academie des Sciences 1962;225:42–3.
[5] Der Kiureghian A, Liu P-L. Structural reliability under incomplete probability information. Journal of Engineering Mechanics, ASCE 1986;112(1):85–104.
[6] Mohr G, Ditlevsen O. Partial summations of stationary sequences of non-gaussian random variables. Probabilistic Engineering Mechanics 1996;11(1):23–5.
[7] Benjamin JR, Cornell CA. Probability, statistics and decision for civil engineers. New York: McGraw-Hill, 1970.
[8] Bishop AW. The use of the slip circle in the analysis of slopes. Proc. 1st European Conf. on Stability of Earth Slopes, Stockholm, 1954:1–13.
[9] Rackwitz R, Peintinger B. Ein wirklichkeitsnahes stochastisches bodenmodell mit unsicheren parametern und anwendung auf die stabilitätsuntersuchung von böschungen. Der Bauingenieur 1981;56(6):215–21.
[10] Peintinger B, Rackwitz R. Numerical uncertainty analysis of slopes. Techn. REp. 52/1980. Munich: LKI, Technical University, 1980.
[11] Hasofer AM, Lind NC. An exact and invariant first order reliability format. J of Eng Mech Div, ASCE 1974;100(EM1):111–21.
[12] Hohenbichler M, Rackwitz R. Non-normal dependent vectors in structural safety. J of the Eng Mech Div, ASCE 1981;107(6):1227–49.
[13] Hohenbichler M, Gollwitzer S, Kruse W, Rackwitz R. New light on first- and second-order reliability methods. Structural Safety 1987;4:267–84.